CHAPTER 2

Airborne remote sensing measurements

The following sections provide a short description of the instruments and the measurement campaign which form the basis of studying cloud radiative smoothing and spatial averaging effects (section 5 and 6, respectively). Additionally, a high-resolution cloudmask is presented which is needed for data preprocessing prior to the analysis of cloud radiative smoothing.

2.1. The airborne research platform of the Institute of Space Sciences

The airborne research platform of the Freie Universität Berlin is a Cessna 207T. In the past the Cessna was modified to allow the installation of diverse remote sensing instruments. The main viewing direction of these instruments is nadir. But after certain modifications, zenith viewing as well as sun tracking can be considered as further options. The nadir viewing instruments are mounted on a stabilised platform, the SM2000 manufactured by Carl Zeiss with a dynamic range of $\pm 8.2^\circ$ (roll), $\pm 6.1^\circ$ (pitch), and $\pm 25^\circ$ (yaw). The permanent equipment of the Cessna comprises of a GPS system, attitude measurements of the platform, and standard meteorological measurements. The Cessna's speed ranges from 80 - 140 kts and its service ceiling is 6000 m.

The instrument park consists of a large variety of remote sensing instruments. The next two sections introduce the two instruments relevant for the analysis presented in this work and provide a detailed description of the calibration procedure.

2.1.1. The compact airborne spectrographic imager. The compact airborne spectrographic imager (*casi*) measures nadir radiances in the visible and near infrared. It is a pushbroom imaging spectrograph using a CCD array as detection unit (see *Babey and Anger* (1989) and *Anger et al.* (1994) for technical details). The two-dimensional array of the CCD comprises of 512 spatial pixels perpendicular to the flight direction and 288 spectral pixels covering a wavelength range of 430-970 nm with a spectral distance $\Delta\lambda$ of 1.9 nm. *Casi* can be operated in three different modes which govern the spatial and spectral resolution and the integration time. If the full frame mode is set, all spatial and spectral pixels are available to perform measurements. Since this mode requires large integration times, it is preferably applied for calibration purposes. The application of the other two modes, the spatial and the spectral mode, should be oriented at the requirements of the actual remote sensing objective. The spatial mode allows measurements with full spatial resolution in up to 19 spectral bands while the spectral mode supports full spectral resolution in up to 39 spatial pixel. In the spectral mode an additional channel, programmable but usually at 753 nm, is available and covers the whole spatial range. The hyperspectral mode is a new enhancement to *casi* and provides the opportunity of increased spectral pixel numbers, maximum 39 bands, by full spatial information. *Casi* has a field of view (FOV) of 0.069° along track and of 34.2° across track. Its dynamic range is 12 bit, and in order to achieve a high degree of saturation, different integration times and apertures (f2 - f16) can be chosen. Usually f2.8 to f8 and integration times between 50 and 150 ms are used during remote sensing experiments. Due to restrictions of *casi*'s applicability with respect to pressure, the maximum flight altitude is reduced to approximately 3500 m.

The spectral and radiometric calibration of *casi* is preferably carried out in the laboratory at the Freie Universität Berlin, prior and past every field experiment. However, it

is recommended to accompany field experiments with calibration measurements at regular intervals to monitor the status of the instrument. An Ulbricht sphere is utilised as light source which has been intercalibrated with a gauged calibration standard. The results presented below are based on an intercalibration with the calibration standard of the Deutscher Wetter Dienst (DWD), Potsdam, Germany. Since 2003, intercalibrations are carried out at FUB due to the acquisition of an appropriate calibration standard.

The spectral calibration relates the spectral channel index to a wavelength. In order to determine the classification five different line lamps, with a varying amount of lines per lamp, oriented at its separability from neighbouring lines, are utilised: three argon, two helium, four hydrogen, three mercury and three oxygen lines. Each measured line is fitted by a Gauss function. The index of the maximum and the full width at half maximum, FWHM, is determined. The index-wavelength dependence is approximated by a polynomial. The spectral calibration from March 2002 yield the following polynomial: λ = 975.26 - 1.9339246 i + 3.7741531x10^{-5} i^2 + 2.6718140x10^{-7} i^3 with i being the spectral pixel number. The relation is almost linear as can be seen by the low factors for orders higher than one. The accuracy of the spectral calibration is defined as the difference between interpolation and sampling points. The maximum difference is 0.8 nm with typical differences below 0.4 nm. FWHM=2.8 nm is determined by the average of five estimates. The spectral characteristics of the lamps are taken from the Atomic Spectra Database, ASD, provided by the National Institute of Standards and Technology, NIST, via Internet: http://physics.nist.gov/PhysRefData/ASD1/.

The overview of the radiometric calibration of *casi* can be outlined as follows:

1) Estimation of an appropriate integration time IT
2) Dark current measurements
3) Absolute measurements
4) Uniform measurements
5) Dark current measurements
6) Estimation of the signal-to-noise ratio SNR

and aims at the determination of calibration coefficients. With the help of these coefficients, the signal, or the digital numbers DN, are converted to units of radiance. All the above mentioned measurements are carried out in full frame mode. The Ulbricht sphere and *casi* must reach operating temperature before calibration measurements can start (~20 minutes). To begin with, the appropriate IT is found if the signal is close to 3/4 of saturation (~3000 DN). This will be the integration time for all subsequent measurements. The dark current measurements before and after the main calibration measurements are done by shadowing the instrument. The dark current is meant to involve the electronic offset EO, which has its origin in the analog electronic of the A/D converter, and the signal arising from thermal effects even though no light is incident on the sensor (usually denoted as dark current, DC). The absolute measurements are taken at a distance of 75 cm, so that approximately 100 spatial pixels are illuminated, and the uniform measurements at a distance of 1 cm. The latter can result in uncertainties due to reflections at the lense what explains the requirement for absolute measurements. The SNR, the ratio of the signal to its standard deviation, is estimated with the help of a specific configuration, a spatial mode with 6 spectral channels and 5000 measurements in total. These measurements are carried out at a distance of 1 cm to the Ulbricht sphere. All other measurements, 2) - 5), should span 512 measurements minimum and must be carried out for each aperture.

Two more phenomena must be considered during the calibration: 1) The reflection of the interior of the grating spectrometer has a significant spectral slope. A shadowed area of the CCD array measures the internally scattered light (SL). 2) During the shift of the measured data to the storage area, light is still incident on the CCD and causes the so called frame shift smear (FSS). The FSS depends on the incident radiation and the duration of the shift, FT, which is approximately 3.84 ms.

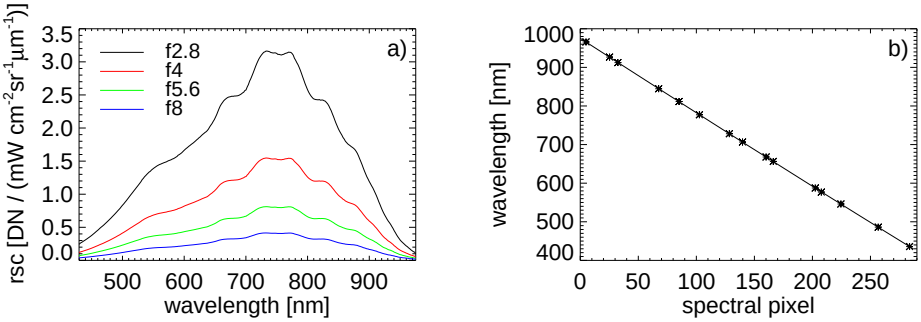

FIGURE 2.1. Results of the radiometric and spectral calibration of *casi*: Calibration coefficients versus wavelength for four different apertures f2.8 - f8 (Fig. a) and relation between spectral pixel number and wavelength (Fig. b). In Fig. b the asterisk mark the sampling points and the solid line the interpolation. The calibration measurements were made in March 2002.

In order to retrieve the calibration coefficients, EO, DC and SL are subtracted from the raw signal R. Then, FSS is estimated by $\mathrm{FT}/\left(288\left(\mathrm{IT}+\mathrm{FT}\right)\right)\sum_i R\left(i,j\right)$ with i being an index of spectral and j of spatial pixels, and is also subtracted from R. This is done for the absolute and uniform measurements. After normalisation on IT, the ratio of the summation of both measurements, using the illuminated pixels only (~100), is multiplied to the uniform measurement. Finally, the ratio of the modified R to the lamp coefficients yields the calibration coefficients rsc (radiant sensitivity coefficients). The lamp coefficients must be carefully interpolated to the spectral channels of *casi*. Akima interpolation (*Akima*, 1970) turned out to be the appropriate tool for interpolation. However, the visual inspection of the interpolation is strongly recommended. Figure 2.1 presents the results of the radiometric and spectral calibration from March 2002. The calibration coefficients, Figure 2.1a, are given for four different apertures, f2.8-f8, as they were frequently used during the BBC campaign (see section 2.2). Figure 2.1b shows the outcome of the spectral calibration, with the sampling points as asterisk and the interpolation as solid line. These results are utilised for the calibration of *casi* data taken during BBC campaign. The maximum possible SNR of *casi* is estimated to be 415:1. It is determined by extrapolation to the maximum possible DN of 4096. The accuracy of the radiometric calibration is affected by the quality of the gauging of the lamp and difficulties in the reproducibility of the calibration set up (various distances and angles as well as a slightly varying power supply of the lamp). The latter argument was addressed by Eyk Bösche and Rasmus Lindstrot, both FUB. These uncertainties accumulate to approximately 3% for visible wavelengths. Additional uncertainties arise from the SNR of the actual measurement. This error, DN / SNR / IT / rsc (in units of radiance), is usually of lower degree since the intensity of cloud reflection is relatively high and IT and aperture are tuned to reach high saturation levels. However, field data at NIR and absorption channels may be affected by noise due to low SNR values at these wavelengths.

Several modes for correcting the radiometric calibration measurements with respect to DC measurements were implemented: direct subtraction of separate DC measurement, interpolation of DC with respect to IT if IT of DC measurement differs from IT of field measurement, interpolation of DC with respect to time if DC measurements before and after the field measurement are available to account for an increase of DC with increasing operation time as well as application of shadowed CCD pixels, if no separate DC measurement is available. A comparison of the effect of the different DC modes on the reproducibility of the lamp spectrum revealed that the direct subtraction should be preferred.

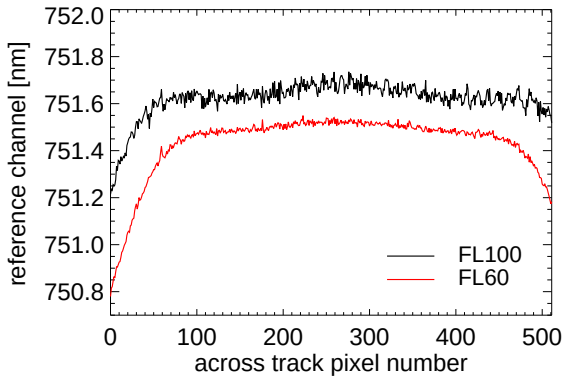

FIGURE 2.2. Inflight spectral calibration of *casi* for two different flight missions: 20 September 2001 (FL100 ~ 3048 m) and 23 September 2001 (FL60 ~ 1829 m).

Some remote sensing applications require very accurate spectral calibrations. An example is the retrieval of cloud top pressure utilising the oxygen A-band absorption. The difficulties arise from the strong increase of absorption intensity around 760 nm. In order to examine the quality of the spectral calibration at the time of the measurement, an inflight spectral calibration of *casi* is carried out. The approach is oriented at the work of *Delwart et al.* (2004). Spectral high-resolution simulations of the nadir reflectance at absorbing channels in cloudless atmospheres were performed with the matrix operator model MOMO (*Fell and Fischer*, 2001) for various sun zenith angles and surface albedos. After convolution of the spectra with *casi*'s spectral response function, assumed to be Gaussian with FWHM=2.8 nm, test and training data sets are provided to an artificial neural network. The network finds an approximation of the relation between the nadir reflectance spectrum around 760 nm and a very accurate spectral position of a reference channel, here at approximately 751 nm. The inversion relies on the characteristic shape of the absorption band. The results of two exemplary spectral inflight calibrations are presented in Figure 2.2. The calibration is carried out for two *casi* observations (20 and 23 September 2001) and clearly revealed a so called smile effect: The spectral calibration shows a relatively strong dependence on the spatial across track pixel. While the relation is almost linear for pixel numbers between 80 and 460, the reference channel declines by up to 0.7 nm at spatial pixel numbers smaller than 80 and, to a lower degree, at pixels larger than 460. Additionally, a significant discrepancy between the spectral inflight calibration of both measurements is observed. At nadir pixels the difference amounts to ~0.2 nm and shows a stronger spatial dependence at FL60. The observed effect may be explained by a temperature dependence of the spectral position of the channel. Radiosonde measurements revealed a temperature of -4 to -5°C and of 2°C on 20 (10:00 and 16:00 UTC) and 23 (9:00 UTC) September 2001, respectively. *Casi*'s possible temperature dependence and the smile effect in combination with a realistic spectral response function are currently topic of a diploma thesis.

2.1.2. FUBISS: Free University Berlin´s Integrated Spectrographic System. FUBISS stands for Free University Berlin´s Integrated Spectrographic System and comprises of a variety of different instruments. Here, the focus is on those spectrometers which are utilised for the investigations presented in subsequent sections.

The FUBISS instruments of interest measure nadir and zenith radiances in different spectral ranges and with different spectral resolutions. FUBISS *vis* measures nadir and zenith radiances between 310 and 1130 nm with $\Delta\lambda$=3.3 nm, FUBISS *highvis* nadir radiances between 600 and 1100 nm with $\Delta\lambda$=0.8 nm, and FUBISS NIR nadir radiances between 950 and 1700 nm with $\Delta\lambda$=6 nm. Each of the instruments consists of a

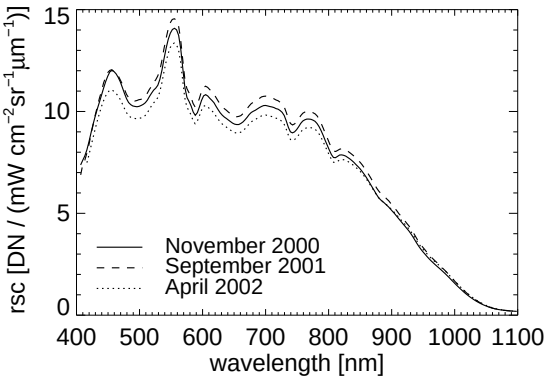

FIGURE 2.3. Comparison of three radiometric calibrations of FUBISS *vis* (nadir). The September 2001 calibration was carried out during the BBC campaign while the other two are conducted in the laboratory.

spectrometer with fixed grating manufactured by Carl Zeiss, a detector from Hamamatsu (S3904 NMOS), an entrance optic, and a fiber optic, connecting the entrance optic and the spectrometer. The NIR measurements are temperature stabilised. All instruments have FOV=5°. Through a user interface, the operator can choose an appropriate IT dependent on the current brightness of the observed target.

The radiometric and spectral calibration procedures are similar to *casi*'s discussed in the previous section: With the exception of the uniform measurements, the same set of measurements must be carried out and is followed by a corresponding data processing to determine the spectral calibration and the calibration coefficients. FSS (and SL) need not to be considered, since the integration time is measured until data readout starts and FUBISS resets its spectrometers before the new measurement starts.

Here, an additional DC mode is available: Provided that the calibration measurements have been carried out at different integration times, they can be interpolated to IT=0 ms which would result in an accurate EO estimate at the time of the measurement. This DC mode is recommended for FUBISS NIR since its observations can be affected by temperature effects which can have significant influences even though the time difference between DC and absolute measurement is small.

Figure 2.3 shows a comparison of three different calibrations carried out in November 2000, September 2001, and April 2002. The September 2001 calibration was conducted during the BBC campaign in the hangar at Rotterdam airport and used to verify the reliability of the instrument. The difference between the other two calibrations averages to 4-5%. The November 2000 results are applied to the FUBISS data received during the BBC campaign, since the difference of these calibration coefficients to the September 2001 coefficients is the smallest. Calibrated field data at wavelengths smaller than 400 nm and larger than 1000 nm should be considered with care, since low instrument sensitivities and/or low lamp intensities may result in large uncertainties. The spectral calibration, here five orders are considered during interpolation, resulted in the following relation for FUBISS *vis*: λ = 308.31747 + 3.2618137 i + 6.5861292x10^{-4} i^2 - 3.7638837x10^{-6} i^3 + 3.5405454x10^{-9} i^4 and FWHM=7.4 nm.

The outcome of the SNR determination is presented in Figure 2.4. The result is received for the FUBISS *vis* (nadir) spectrometer and shows considerably higher SNR values, if compared to *casi*'s values. Starting at 850 nm, the SNR drops rapidly with increasing wavelength. The maximum achievable SNR is ~4400 for a maximum DN of 32768 (16 Bit converter).

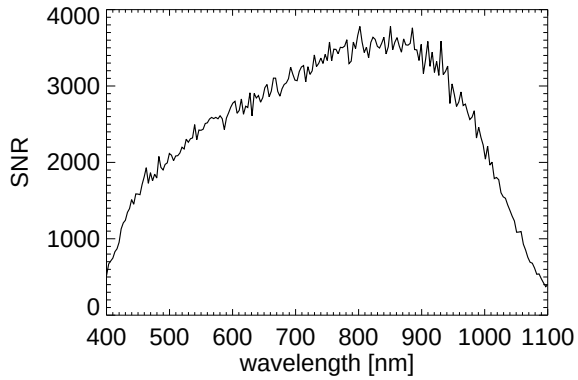

FIGURE 2.4. Signal-noise ratio (SNR) of the FUBISS *vis* (nadir) spectrometer versus wavelength. Note the strong decrease of SNR at wavelengths larger than 850 nm.

The radiometric accuracy of FUBISS *vis* and *highvis* is higher compared to *casi*'s due to the significantly larger SNR. The uncertainty of the spectral calibration is estimated to be <0.3 nm.

2.2. The Baltex Bridge Cloud (BBC) campaign

The Baltex Bridge Cloud (BBC) campaign took place in Cabauw, The Netherlands, from 3 until 28 September 2001. The BBC campaign was a joint venture of the German 4D-Clouds and the European Cliwa-Net project. The main objective of 4D-Clouds aims at the improved understanding of the effect of inhomogeneous cloud structure on the transport and exchange processes in the atmosphere. Especially, open issues concerning enhanced absorption are investigated. During the experiment coordinated observations of clouds by various ground based and remote sensing sensors were carried out. A network of seven ground stations was set up where each station was equipped at minimum with lidar, pyranometer, infrared and microwave radiometers. Additionally the standard instrumentation of the weather service of The Netherlands plus cloud radars are situated at the Cabauw station. Three aircrafts were operated to measure cloud microphysics and radiation below, within and above clouds and are accompanied by satellite observations. An overview of the experiment including introductions to utilised instruments and first results is given by *Crewell et al.* (2004). The major interest of the Freie Universität Berlin (FUB) was the systematic investigation of the effect of three dimensional cloud structure on atmospheric radiation and the identification of scale dependencies related to this effect. In order to address the objectives, it participated with its airborne research platform, the Cessna 207T. A list of instruments mounted to the Cessna together with a short description of the instruments is given in Table 2.1. During the measurements the attitude stabilisation was active for the nadir looking instruments. FUBISS *extended* performed first test measurements which made the need for stabilisation, on board DC measurements and the prevention of water condensation obvious. During the entire campaign FUBISS NIR and MIDAC did not operate reliable after installation into the aircraft due to technical defects. The HDRAD data was successfully processed at FUB and submitted to the Universität Heidelberg. FUBISS *vis* and *casi* measurements form the basis of the observational results presented in this work.

During the campaign a total of 13 flights were performed with the Cessna 207T. An overview of the flight tracks is given in Figure 2.5. Flight tracks and appropriate dates are colour coded, and with one exception, all flight patterns are horizontal, straight legs between the ground stations. These stations are marked with S1 to S7, and S1 is Cabauw.

TABLE 2.1. lnstrumentation of the Cessna during BBC.

Instrument	Description
casi	Compact airborne spectrographic imager, nadir radiances (490 - 900 nm)
FUBISS *vis*	FUB's Integrated Spectrographic System, nadir and zenith radiances (310 - 1130 nm)
FUBISS *highvis*	nadir radiances (600 - 1100 nm)
FUBISS NIR	nadir radiances (950 - 1700 nm)
FUBISS *extended*	upward and downward irradiances (400 - 1000 nm)
HDRAD	Radiometer from the Universität Heidelberg, nadir radiances (4 visible channels)
MIDAC	Fourierspectrometer, nadir radiances (5-17 μm)

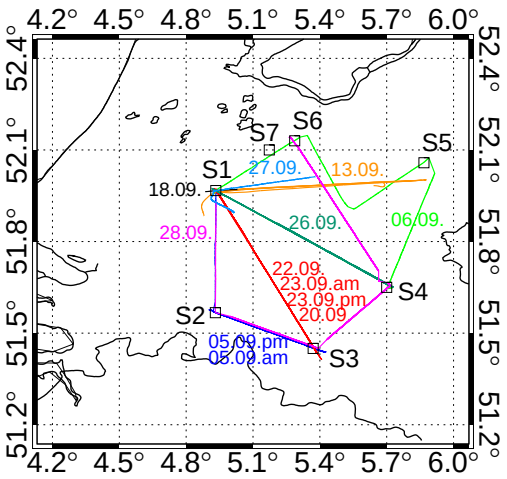

FIGURE 2.5. Overview of flight missions carried out during BBC. The colour coding of the flight dates corresponds to the colour of each flight mission. The squares present the ground stations S1-S7, with S1 being Cabauw.

The dates as well as start and stop times of each flight mission are provided in Table 2.2. The flight altitude varied between 1520 and 3350 m and the duration between 0.5 and 2 hours. The distance between aircraft and cloud was highly variable, and occasionally the aircraft was in clouds.

During the BBC campaign *casi* was configured to achieve highest spatial resolution with a maximum amount of spectral channels. To achieve this, *casi* was operated in hyperspectral mode. 37 spectral channels have been defined in wavelength ranges relevant for remote sensing. Figure 2.6 shows an exemplary near true colour image made with *casi*. It was recorded on 22 September 2001 and demonstrates the small scale variability of clouds and underlying surfaces.

In order to verify the observations made by FUBISS *vis* and *highvis* as well as *casi*, the calibrated signals received by the instruments were compared. Figure 2.7 shows the outcome: Figure 2.7a the spectral and Figure 2.7b the time series comparison at 10.223 UTC and for a wavelength of 753 nm, respectively. If the different integration times, the unsynchronised measurements, the different FOV, different channel definitions and possible

TABLE 2.2. Date, start and stop times of conducted flight missions during BBC.

Date	Start time [UTC]	Stop time [UTC]
05 September 2001	09:16	09:56
06 September 2001	13:12	14:08
13 September 2001	09:48	10:55
18 September 2001	09:27	11:07
20 September 2001	12:12	13:38
22 September 2001	09:02	10:25
23 September 2001	08:45	10:30
23 September 2001	12:50	14:57
25 September 2001	13:45	14:46
26 September 2001	09:52	10:35
27 September 2001	09:30	10:18
28 September 2001	09:31	10:22

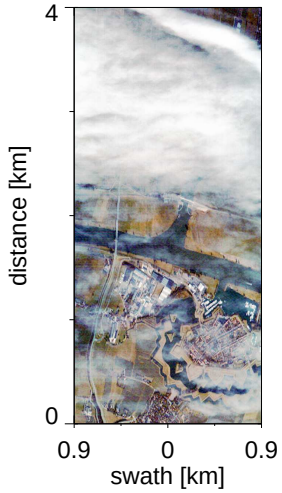

FIGURE 2.6. *Casi* near true colour image. The data was recorded on 22 September 2001.

deviations from nadir view are kept in mind, the agreement between the plots is excellent. Due to different instrument set ups in combination with the inhomogeneity of clouds the discrepancy between the signals can reach values of up to 45% if time series at 753 nm are considered (not shown).

All *casi* images at 753 nm were divided in sections of 10 km length resulting in a total amount of ~250 images. Together with the date of the flight mission, the start and stop time of each leg, and track overview plots, showing flight direction, location of each section and its length as well as position relative to ground stations, the images are summarised in the BBC 2001 *casi* data catalog. The catalog provides an excellent overview and a quick impression of the current cloud or surface situation.

Due to extremely rainy weather during BBC a second BBC campaign, the BBC2 campaign, was carried out with similar objectives in May 2003. Additionally, a validation experiment is currently conducted to validate the retrieval of cloud top height from satellite measurements. A Lidar from the Universität München and *casi* was mounted to the Cessna 207T for the validation. The cloud top height retrieval from *casi* observations is currently the topic of a diploma thesis at FUB.

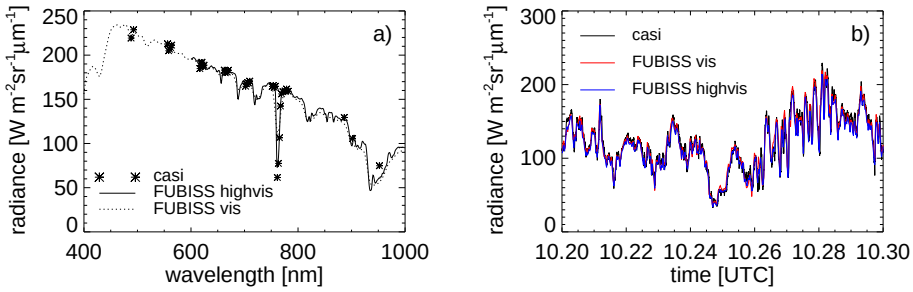

FIGURE 2.7. Spectral (Fig. a) and time series (Fig. b) comparison of calibrated *casi*, FUBISS *vis* and *highvis* observations. The spectra are taken at 10.223 UTC, and the time series is compared at 753 nm. The times are given as floating point.

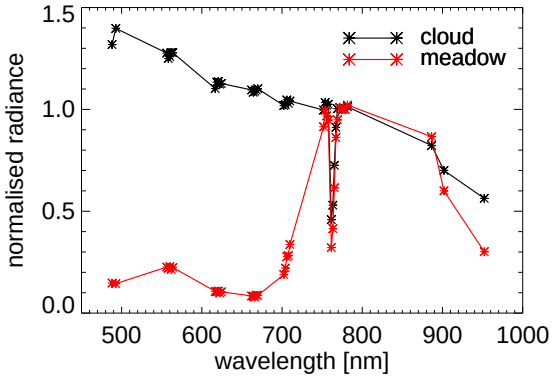

FIGURE 2.8. Normalised radiance versus wavelength for two different underlying targets (cloud and meadow). Besides absorption features of water vapour and oxygen, the rededge is clearly visible at wavelengths larger than 700 nm. The normalisation is done to the radiance at 780 nm, and the spectra are taken from 13 September 2001.

2.3. Generating cloudmasks in spatial high-resolution observations

Cloud detection from remote sensing is required for many applications: the determination of cloud cover, the identification of cloudy pixels for the retrieval of cloud related parameters, or the exclusion of pixels with even minor cloud contamination if further processing would be affected by the presence of clouds, e.g. for land surface, ocean color, and aerosol observations.

During the BBC campaign high spatial-resolution measurements over land surfaces were performed with *casi* (section 2.1). In order to analyse cloud radiative smoothing (section 5) a complete cloud coverage should be guaranteed to exclude signals related to land surface.

The basic idea behind the cloudmask generation is the strong increase of plant reflectivity at wavelengths around 700 nm, referred to as the red edge. Figure 2.8 provides an impression of this increase by plotting the radiance measured over meadow normalised to a reference channel at 780 nm. Additionally, the normalised radiance received over a cloud is shown for comparison (data from 13 September 2001). Estimates of the surface albedo,

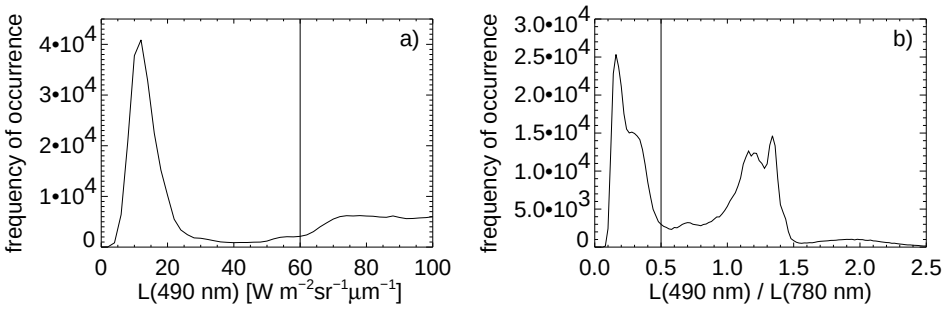

FIGURE 2.9. Histograms of the radiance L at 490 nm (Fig. a) and of the ratio of the radiances at 490 nm to 780 nm (Fig. b). The total number of data points sums up to more than $5\text{x}10^5$. The maximum radiance of 435 W $\mathrm{m}^{-2}\mathrm{sr}^{-1}\mu\mathrm{m}^{-1}$ is not shown in Fig. a. The vertical lines indicate the thresholds as used in the cloudmask algorithm. The radiances was recorded on 13 September 2001.

retrieved from airborne irradiance measurements during the BBC campaign, are presented by *Wendisch et al.* (2004).

In order to separate cloudy from cloudfree pixels, the radiative effect of the red edge is parameterised by the ratio of radiances at 490 nm and 780 nm. Additionally, the low reflectivity of plants around 490 nm stands in contrast to high reflectivities of clouds at this wavelength and therefore yields to the application of absolute radiances at 490 nm. The histograms of a series of *casi* images, showing broken cloud fields, are analysed to find appropriate thresholds to separate cloudy from cloudfree pixels. Figure 2.9 shows an example of the threshold identification for data received on 13 September 2001. The histograms of L(490 nm) (Fig. 2.9a) and of the ratio (Fig. 2.9b) are presented together with the final thresholds which are indicated by vertical lines. The thresholds are 0.5 and 60 W $\mathrm{m}^{-2}\mathrm{sr}^{-1}\mu\mathrm{m}^{-1}$ for the ratio and L(490 nm), respectively. If both values of a single pixel are larger than these thresholds the pixel is detected as cloudy. Since independent observations for a verification of the cloudmask are not available, the thresholds are slightly adjusted after visual inspection of several cloudmasks and corresponding radiance images. Tuning to lower values generally increases the cloud fraction because more thin clouds are successfully and more surface pixels are falsely detected and vice versa for tuning to higher thresholds. Since the cloudmask is developed for the preprocessing of *casi* data for statistical analysis which requires cloudy images, an underestimation of cloud fraction is favoured over a misinterpretation of cloudfree pixels (see section 5.1).

The application of this cloudmask algorithm can be problematic if a cloudshadow falls on top another cloud. So affected cloud pixels are characterised by low radiance intensities but high ratios and are identified as cloudfree in several images. These cases have not been observed infrequently as can be read in the flight log. In order to avoid such misidentifications a second threshold combination is introduced: The pixel is detected as cloudy if the ratio is larger than 1.35 and L(490 nm) is larger than 35 W $\mathrm{m}^{-2}\mathrm{sr}^{-1}\mu\mathrm{m}^{-1}$. The second threshold is applied in case the pixel is identified uncloudy by the first threshold. The effectiveness and the necessity are demonstrated in Figure 2.10. The left panel provides an enhanced *casi* image recorded on 13 September 2001, which is opposed by the cloudmask (middle panel). The greyscales of the cloudmask are as follows: White marks cloudy pixels after application of the first two thresholds only, while grey indicates cloudy pixels which are identified cloudy after application of the second pair of thresholds. Black pixels represent the remaining cloudfree parts. The red circle marks the position of the spectrum shown in the right panel. Both, the left and the right panel verify the assumption that large

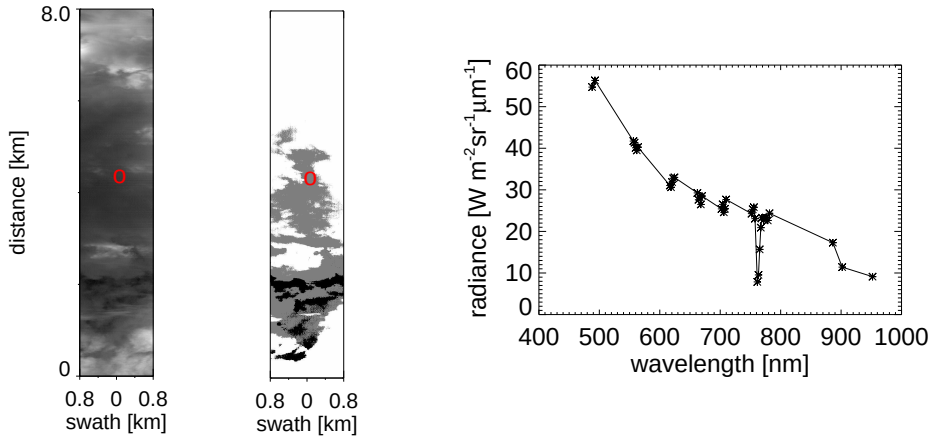

FIGURE 2.10. The necessity and the effectiveness of the application of a second pair of thresholds to derive cloudiness are demonstrated. The left panel shows an enhanced *casi* image (13 September 2001). The middle panel presents the corresponding cloudmask with the following greyscales: Black stands for cloudfree, white for cloudy pixels after application of the first two thresholds and grey for cloudy pixels identified with the help of the second pair of thresholds. The red circle marks the position of the spectrum given in the right panel.

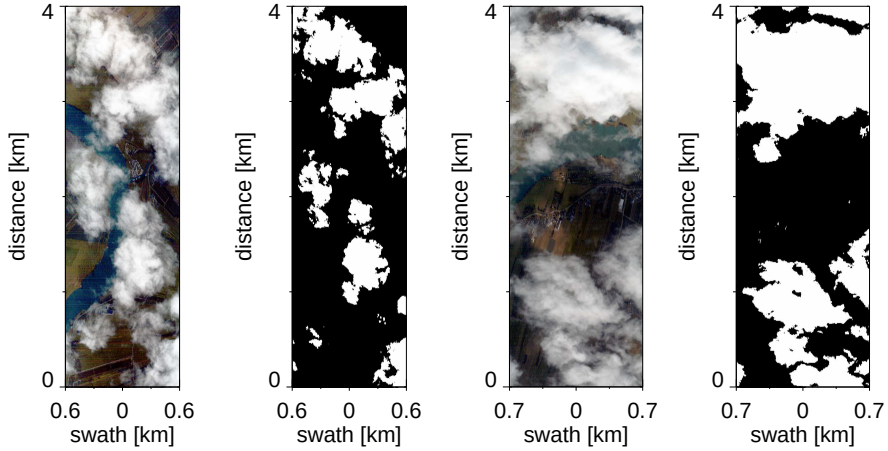

FIGURE 2.11. Exemplary near true colour *casi* images and cloudmasks from 18 (left panels) and 23 (right panels) September 2001. Both *casi* images, first and third panel, show broken cloud fields over land surfaces of various kind. The spatial high resolution cloudmasks, white corresponds to cloudy pixels, show a relatively high quality.

parts of the darker regions in the left panel are indeed cloud shadows on top clouds. The second threshold pair obviously improved the quality of the cloudmask.

Figure 2.11 shows two exemplary near true colour *casi* images (first and third panel) with corresponding cloudmasks (second and fourth panel). The *casi* images haven been enhanced and are taken from 18 (first panel) and 23 (third panel) September 2001 with maximum radiances of 156 and 223 W $\mathrm{m}^{-2}\mathrm{sr}^{-1}\mu\mathrm{m}^{-1}$, respectively. White parts of the cloudmasks are related to cloudy and black to cloudfree parts. The accuracy of both cloudmask examples is relatively high. The major problems arise from cloud edges and relatively thin cloud parts which remain undetected as can be seen in the left two panels in particular.

Minor misinterpretations can emerge from surfaces characterised by high albedos. These surfaces can be sand, glasshouses, boats, and others. An example can be seen in the right two panels where falsely identified pixels can be found at a distance of 1.5 to 2 km. If the cloud fraction of this exampple and other cases is determined, the related uncertainty is usually small since the affected area is small compared to the spatial coverage of the whole image.

The cloudmask and the cloud fraction was determined for each section of the BBC 2001 *casi* catalog, see previous section. The overall performance of the cloudmask is more than sufficient, especially, if the simplicity of the algorithm, the patchy like structure of thin cloud parts and its usage for preprocessing (section 5.1) are seen.

Schröder et al. (2002) discuss a cloudmask for spatial high-resolution observations over oceans which are affected by sunglint to large degrees in intensity and amount. The generation of the cloudmask relies on an automated artificial neural network fed with absolute radiances, gradient filters, and texture information. The latter proved to be sensible to the high frequencies observed in sunglint areas which stands in contrast to the comparatively low variability of the signal received over clouds.